Normal Variants and Pitfalls in MR Imaging of the Ankle and Foot

Soterios Gyftopoulos, MD[a], Jenny T. Bencardino, MD[b,*]

KEYWORDS

• MR Imaging • Ankle • Foot • Variants • Pitfalls

MR OF THE MUSCULOSKELETAL STRUCTURE

Great advances have been made in musculoskeletal radiology since the dawn of cross-sectional imaging more than three decades ago. Innovation in imaging technology has provided an unprecedented window into intra-articular pathology. MR imaging, in particular, has revolutionized the ability to study the anatomic details of all the components of the musculoskeletal system, including tendons, ligaments, muscles, and bones as well as the pathologic processes that affect them. Crucial to the accurate analysis of these structures is a solid knowledge of the anatomic variants that can be misinterpreted for pathology on MR imaging. This article focuses on the variants and imaging pitfalls in the ankle and foot.

TECHNICAL FACTORS

As a general rule, the tendons and ligaments of the ankle and foot, due to their highly organized architecture and collagen composition, demonstrate homogeneously hypointense signal on all pulse sequences. Loss of the expected low intrasubstance signal in a tendon or ligament is considered the hallmark in the diagnosis of pathologic conditions. The magic angle phenomenon is a technical phenomenon that can mimic pathology. The magic angle effect occurs when the orientation of the collagen fibers approximates the magic angle of 55° with the main magnetic vector (Z axis). This phenomenon is particularly prominent when a low echo time (TE) of 10 to 20 milliseconds is used, as in T1-weighted, proton density, and gradient-echo sequences. T2-weighted or short tau inversion recovery (STIR) images with high TE values (>35 milliseconds) eliminate the magic angle effect. When imaging the ankle, this phenomenon can be reduced by scanning patients in the prone position or positioning the foot at 20° of plantar flexion while scanning patients in a supine position. The magic angle more frequently affects the posterior tibial tendon just proximal to its navicular insertion, the peroneal tendons in subfibular position, and the anterior tendons at the level of the ankle joint (**Figs. 1** and **2**).

Incomplete fat suppression can falsely produce hyperintense signal in the soft tissues and bone marrow, most commonly in the lateral aspect of the ankle in the region of the lateral malleolus, although the medial malleolus can also be affected (**Fig. 3**). This is thought to be due to factors, such as coil proximity artifact and the presence of inhomogeneities in the static magnetic field. Inhomogeneous fat saturation can be combated through the use of inversion recovery imaging, which is insensitive to field inhomogenities, and by the use of multichannel phase array coils.

TENDONS

Anterior Compartment

The anterior compartment tendons (anterior tibial, extensor hallucis longus, extensor digitorum longus, and peroneus tertius) are rarely injured. The anterior tibial tendon is the most commonly injured

[a] Department of Radiology, NYU Hospital for Joint Diseases, New York, NY 10003, USA
[b] Department of Radiology, NYU Hospital for Joint Diseases, 310 East 17th Street Sixth Floor, New York, NY 10003, USA
* Corresponding author.
E-mail address: Jenny.bencardino@nyumc.org

Magn Reson Imaging Clin N Am 18 (2010) 691–705
doi:10.1016/j.mric.2010.07.007
1064-9689/10/$ – see front matter

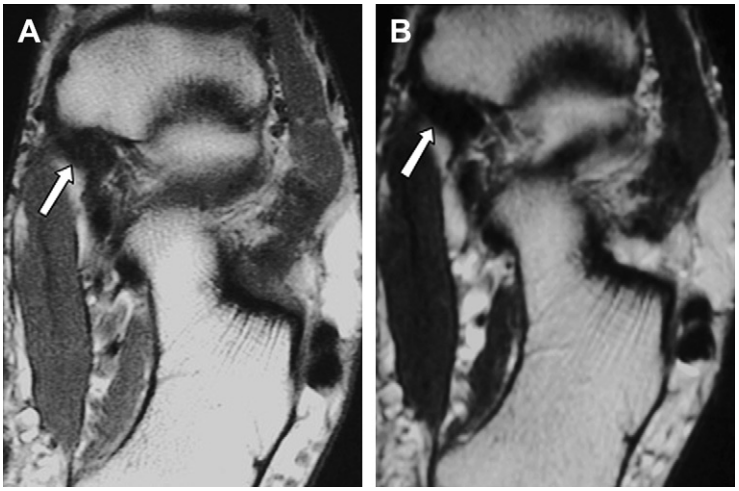

Fig. 1. Magic angle phenomenon is demonstrated on the axial T1-weighted image (*A*) as intrasubstance intermediate signal within the insertional fibers of the posterior tibial tendon (*white arrow*), which entirely disappears on the fast spin-echo T2-weighted image (*B*).

extensor tendon. Tear of the anterior tibial tendon is classically seen in older patients and athletes who run hills.[1] Apparent longitudinal split tearing in the insertional portion of this tendon at the medial cuneiform bone and base of the first metatarsal in asymptomatic patients is most likely related to the presence of multiple insertional slips. This is thought to represent a normal variant.[2]

Medial Compartment

The insertional portion of the posterior tibial tendon on the medial navicular tubercle typically has a heterogenous appearance. This signal heterogeneity is secondary to a combination of magic angle effect and fat interposed between the insertional slips of the tendon.[3,4] Another cause of the heterogeneity is the presence of an intratendinous accessory navicular bone (type I accessory navicular bone [os tibiale externum]) (**Fig. 4**).[5]

A small amount of tenosynovial fluid is frequently observed within the tendon sheaths in asymptomatic individuals and should not be considered abnormal. Physiologic tenosynovial fluid is more frequently found in the flexor than in the extensor tendons.[6] The lack of tendon sheath in the distal preinsertional portion of the posterior tibial tendon renders fluid signal in this location abnormal, however. Posterior tibial peritendinitis likely related to metaplastic synovium should be considered.[6] Disproportionate fluid within the flexor tendon sheaths, compared with the amount of fluid found in the ankle joint, is usually indicative of tenosynovitis. Communication between the ankle joint and the flexor hallucis longus tendon, however, explains the presence of prominent fluid within this tendon sheath in patients with large joint effusions. Thus, even a large amount of fluid within

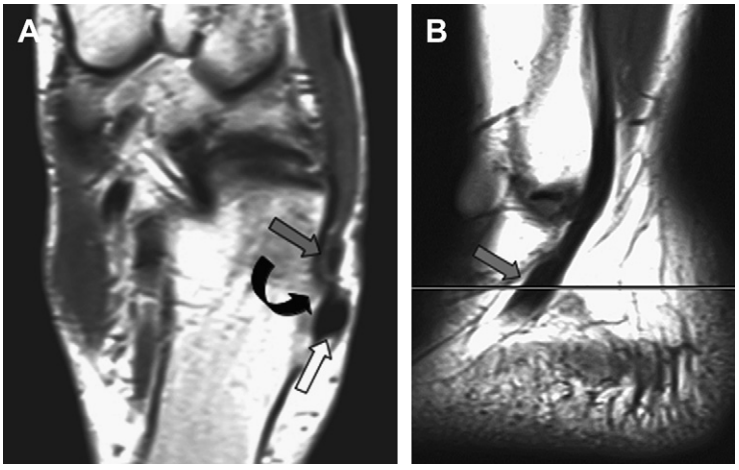

Fig. 2. Axial proton density (*A*) and sagittal T1-weighted (*B*) images demonstrate high signal within the peroneus brevis tendon (*gray arrow*) at the level of the peroneal tubercle (*curved arrow*) of the lateral calcaneal wall related to magic angle phenomenon (*arrows*). The peroneus longus tendon (*white arrow*) is not affected because it is coursing more vertically with respect to the peroneus brevis tendon at this level.

Fig. 3. Coronal, fat-suppressed, T2-weighted image of the ankle demonstrates inhomogenous fat suppression resulting in spurious increased signal in the lateral and medial malleoli and overlying soft tissues (*arrows*).

Fig. 4. Axial intermediate image of the ankle demonstrates a type I accessory navicular (*gray arrow*) embedded within the posterior tibial tendon (*white arrow*).

the tendon sheath of the flexor hallucis longus tendon may be of no clinical significance.[6]

Posterior Compartment

The tendons of the gastrocnemius and soleus muscles form the Achilles tendon. The Achilles tendon measures approximately 15 cm in length and typically has a fascicular appearance secondary to the intermixing of its fibers with fibrofatty tissue and vessels. This, in turn, produces intrasubstance linear and punctate hyperintense foci on T1-weighted and gradient-echo images.[7] Preservation of the normal morphology of the tendon helps differentiate this signal heterogeneity from a partial tear because a normal tendon maintains its normal flat/concave shape anteriorly and demonstrates intact fibers throughout its course without intervening fluid-like T2 signal. In addition, the fascicular appearance is usually less apparent on STIR and T2-weighted images.[8,9]

Low or incomplete incorporation of the gastrocnemius and soleus tendons may produce heterogeneity due to persistent fat planes between the tendon slips. Assessment of the course of the soleus tendon relative to the gastrocnemius tendon on sequential axial images avoids confusing this normal variant with disease (**Fig. 5**).[10] A pathologic process that can mimic this appearance is a xanthomatous Achilles tendon. Xanthomas are composed of lipid-filled foamy histiocytes and extracellular cholesterol deposits. They are typically seen in patients with inherited metabolic diseases, such as familial hypercholesterolemia and hyperproteinemia.[11,12] A xanthomatous Achilles tendon typically has a speckled or reticulated appearance with or without tendon enlargement.[12] This MR imaging appearance correlated with a patient's medical history helps diagnose this pathologic process.

Lateral Compartment

The peroneal tendons (peroneus brevis and peroneus longus) share a common tendon sheath down to the level of the lateral malleolar tip. From this point on, the tendons have individual tendon sheaths. The peroneal tendons can be affected by magic angle effect because they course obliquely around the lateral malleolus and onto their insertions in the foot, particularly as the peroneus longus tendon curves beneath the cuboid bone. The primary restraints to subluxation of the peroneal tendons are the superior and inferior peroneal retinacula. The superior peroneal retinaculum courses from the posterolateral aspect of the distal fibula to the lateral calcaneus and helps stabilize the tendons in the retromalleolar groove.

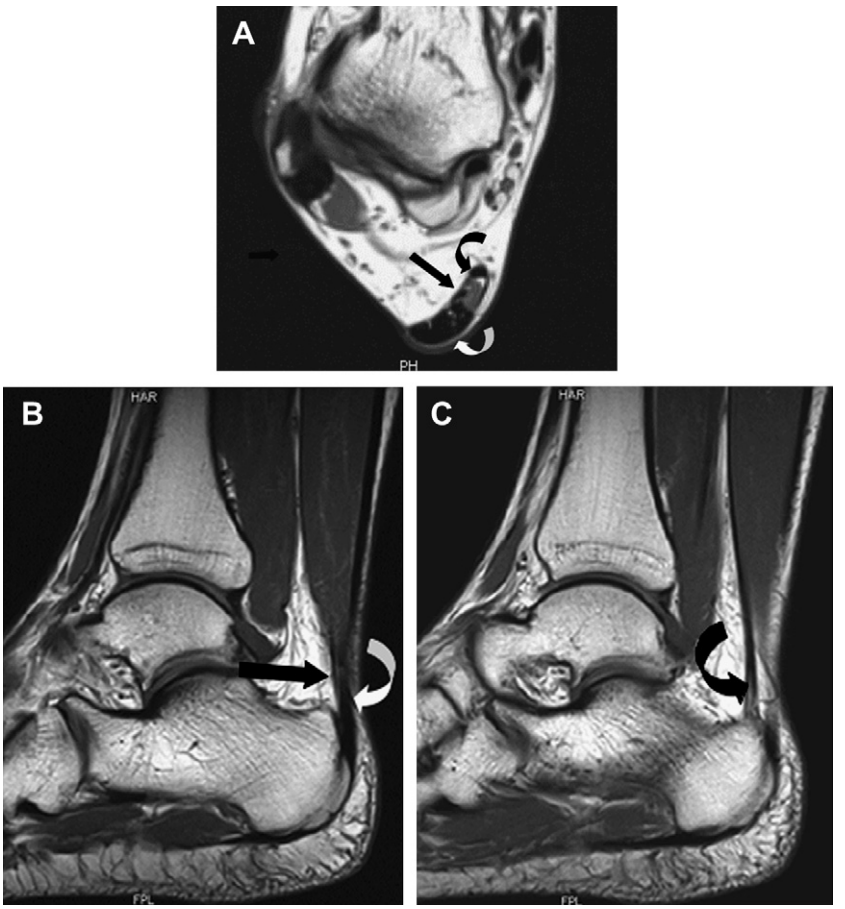

Fig. 5. Axial proton density–weighted (*A*) and sagittal T1-weighted (*B, C*) images at the level of the distal Achilles tendon (*curved white arrow*) demonstrates a low incorporating soleus (*straight arrow*) as well as a separate accessory soleus tendon (*curved black arrow*) inserting into the posteromedial calcaneus.

The inferior peroneal retinaculum attaches to the peroneal trochlea and calcaneus above and below the tendons while forming a septum that reinforces the individual tendon sheaths. The oblique course of the peroneus brevis tendon leads to apparent subluxation of the tendon where the brevis tendon is found medial to the medial margin of the fibular groove instead of at its more frequent position posterior to the fibular groove and anterior to the peroneus longus tendon. Pseudosubluxation of the peroneus brevis tendon can be further accentuated in foot supination.[13]

LIGAMENTS

Lateral Compartment

Of the three main ligaments in the low lateral compartment of the ankle, the least prone to injury is the posterior talofibular ligament. This ligament tends to have a fan-like, striated appearance on MR imaging that should not be confused with a sprain or tear.[4,14] The posterior talofibular ligament and the posterior intermalleolar ligament course transversely posterior to the tibiotalar joint and, thus, frequently appear as punctuate hypointensities as they are imaged in cross section in the sagittal plane. This appearance can mimic posterior ankle intra-articular bodies. It is important to carefully track each of these ligaments from their origin to insertion to exclude the presence of a loose body using the orthogonal imaging planes.[4,14]

Syndesmotic Ligaments

The anterior tibiofibular ligament can also pose a diagnostic dilemma, because it may appear thickened and discontinuous. This appearance can be a normal finding and is thought to be related to fat interposed between the fibers that make up the ligament as well as due to its downward oblique orientation from the anterior tibial lip to its insertion into the fibular malleolus

(Fig. 6). As with the posterior intermalleolar and posterior talofibular ligaments (discussed previously), the anterior and posterior tibiofibular ligaments can mimic intra-articular loose bodies on the sagittal plane due to their transverse course.[4,14]

Medial Compartment

The deltoid ligament complex is made up of superficial and deep layers. One of the most readily visualized components of the complex is the posterior tibiotalar ligament, a component of the deep layer. This ligament has a striated appearance due to the presence of intervening fat between its fibers, which should not be confused with injury. This striated appearance is regularly seen in the young adult population.[4,14,15]

The spring ligament complex is made up of three separate components: the superomedial, the medial plantar oblique, and the inferior plantar longitudinal fibers. The spring ligament complex is an important structure of the anterior subtalar joint providing a fibrocartilaginous articular surface to the talar head (Fig. 7A). The superomedial component, which courses from the medial aspect of the sustentaculum tali to the superomedial aspect of the navicular, runs medial to the distal posterior tibial tendon and is separated by loose connective tissue.[16] This loose connective tissue helps differentiate between the posterior tibial tendon and superomedial spring ligament. Frequently noted between the medial plantar oblique and the inferior plantar longitudinal ligaments is a fluid-filled recess of the talocalcaneonavicular (Fig. 7B). Fluid signal within this recess may potentially be misconstrued as a spring ligament tear. Visualization of the recess is facilitated by the presence of a native effusion or by intra-articular injection of contrast solution in the talonavicular joint. Posttraumatic talonavicular effusions in the setting of acute impaction injury of the talar head and talonavicular osteoarthritis are often seen in association with a fluid distended spring recess.[17]

Accessory Ligaments

The posterior intermalleolar ligament is a ligament found in the posterior aspect of the ankle in 81.8% of specimens.[18] It was originally described as a ligamentous structure extending between the medial malleolus and the lateral malleolus (Fig. 8). Recent studies have reported a diverse group of medial origins with the lateral insertion consistently found in the medial fossa of the lateral malleolus.[18] This ligament can have different shapes depending on the site of its medial origin as well as of the number of fiber bundles and their density. The posterior intermalleolar ligament can potentially become entrapped and be a cause of posterior ankle impingement.[19]

In general, it is important to correlate the clinical history along with the imaging findings when evaluating these structures for injury. The morphology of each ligament and tendon should be carefully examined as well as its signal in conjunction with the status of the surrounding soft tissue and osseous structures to confidently differentiate a tear or sprain from a normal variant.

MUSCLES

Muscle variants are frequently seen in the ankle.[4,14,20,21] These muscles are usually asymptomatic and often incidentally found on MR imaging obtained for unrelated reasons. When they do come to attention, they can either present as a mass on physical examination or cause pain related to their effect on the surrounding structures.[20,21] For instance, the peroneal tunnel can house an accessory muscle, the peroneus quartus, which is located adjacent to the peroneus brevis and peroneus longus tendons. This muscle can cause peroneal tunnel overcrowding, leading to

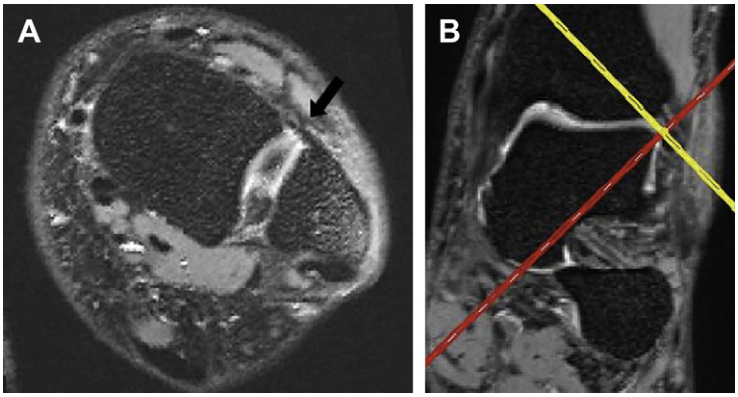

Fig. 6. Axial, oblique, fat-suppressed, proton density, 3-D reconstructed image (*A*) demonstrates the anterior tibiofibular ligament in its entirety (*arrow*). (*B*) Coronal, oblique, proton density, source 3-D image.

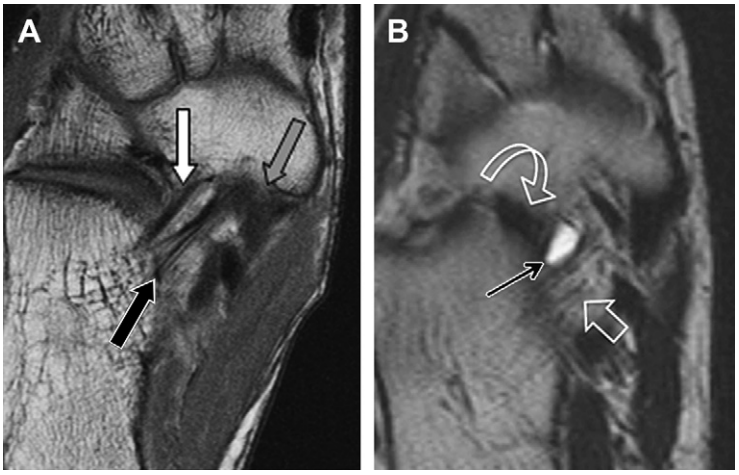

Fig. 7. (*A*) Axial intermediate-weighted image of the ankle demonstrates the medioplantar oblique (*black arrow*) and inferoplantar longitudinal (*white arrow*) components of the spring ligament complex normally found at the level of the posterior tibial tendon attachment on the medial navicular tubercle (*gray arrow*). (*B*) Axial fast spin echo T2-weighted image demonstrates a fluid filled spring ligament recess (*black arrow*) interposed between the medioplantar oblique (*open arrow*) and inferoplantar longitudinal (*curve arrow*) components.

mass effect and compression on the peroneus brevis and peroneus longus tendons and eventual tearing.[22] The peroneus quartus inserts independently into the retrotrochlear eminence of the lateral calcaneus, which helps differentiate it from a low-lying peroneus brevis muscle belly (**Fig. 9**). The latter, unlike the peroneus quartus, does not predispose to tearing. The flexor accessorius digitorum longus (FADL) is the most common accessory muscle found within the tarsal tunnel. Due to its location inside the tarsal tunnel, the FADL can cause mass effect on the adjacent tibial nerve or its plantar branches, particularly during exercise-related engorgement leading to neuropathy and denervation (**Fig. 10**).[23] Other common normal muscle variants include the accessory soleus,[24,25] low incorporation of the soleus, and peroneo calcaneus internus muscles. An accessory soleus can be distinguished from low incorporation of the soleus by following the course of the tendon in question. The tendon of the accessory soleus inserts separately onto the calcaneus anteromedial to the attachment of the Achilles.[26]

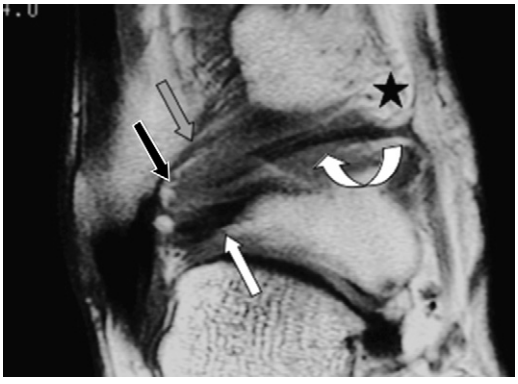

Fig. 8. Coronal intermediate-weighted image demonstrating the posterior intermalleolar ligament (*curved white arrow*) extending from the posterior margin of the medial malleolus (*star*) to the lateral malleolar fovea (*black arrow*) interposed between the inferior band of the posterior tibiofibular ligament (*gray arrow*) and the posterior talofibular ligament (*white arrow*).

BONES

There are various normal anatomic variants and pitfalls related to the osseous structures of the ankle and foot. Similar to the evaluation of the ligaments and tendons, it is important to not only be familiar with these variants but also use the information in the surrounding structures to make an accurate diagnosis.

Os Variants

Ossicles or secondary ossifications centers can be found in various locations of the foot and ankle. They are usually asymptomatic, but it is important to not confuse them with a fracture fragment or tumor of osseous origin. This can be avoided by knowing their typical location, configuration, and size.

In the medial ankle compartment, the most frequently found accessory ossicle is the os naviculare. Three types have been described, each with its own characteristic imaging appearance and clinical significance.[27] A type I accessory navicular ossicle or os tibiale externum is found embedded in the distal portion of the posterior tibial tendon. It has a round or oval shape, can measure between 2 to 6 mm in diameter, and is usually located up to 5 mm proximal to the medial navicular tubercle (see **Fig. 4**). A type I accessory navicular is typically of no clinical significance. The ossicle typically follows the MR imaging

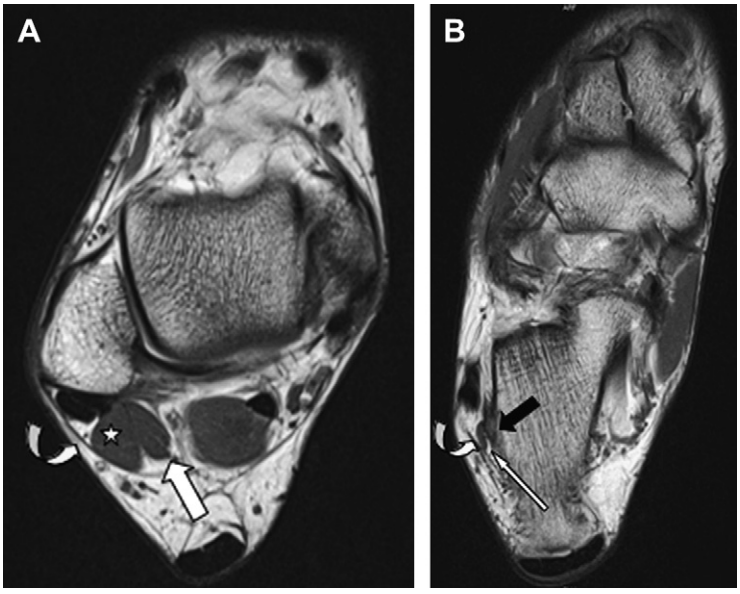

Fig. 9. Axial intermediate-weighted images (*A, B*) demonstrate a peroneus quartus muscle (*white arrow*) descending within the peroneal tunnel along the medial aspect of the peroneus brevis muscle (*asterisk*). Note the conjoint insertion of the peroneus quartus onto the retrotrochlear eminence (*black arrow*) with the inferior peroneal retinaculum (*curved white arrow)*.

characteristics of bone marrow with a thin cortical hypointense margin. A type II accessory navicular ossicle has a triangular shape, and is attached to the medial navicular via a cartilaginous and/or fibrous syndesmosis. It can serve as the main site of attachment for the posterior tibial tendon, which in turn, may cause stress at the synchondrosis. This can present, clinically, as medial-sided midfoot pain. MR imaging can demonstrate T2 hyperintense signal within the synchondrosis, accessory navicular, medial navicular tuberosity, and surrounding soft tissues, representing edema, in what is known as symptomatic accessory navicular syndrome.[4,28] A type III accessory ossicle has a complete osseous fusion and incorporation to the navicular bone, creating a horn-like or cornuate navicular. This type of ossicle serves as an attachment site for the posterior tibial tendon reducing the distance between the lateral malleolus fulcrum and the medial navicular insertion. This is thought to increase biomechanical stress in the tendon fibers, increasing the risk of tendinosis and tear (**Fig. 11**).[29]

The lateral compartment contains the os peroneum, an accessory ossicle embedded within the tendon of the peroneus longus tendon. This ossicle is regularly seen in primates related to the peroneus longus tendon role in hallux adduction.[30] In humans, the os peroneum is found in 20% of the population and serves no functional purpose.[31]

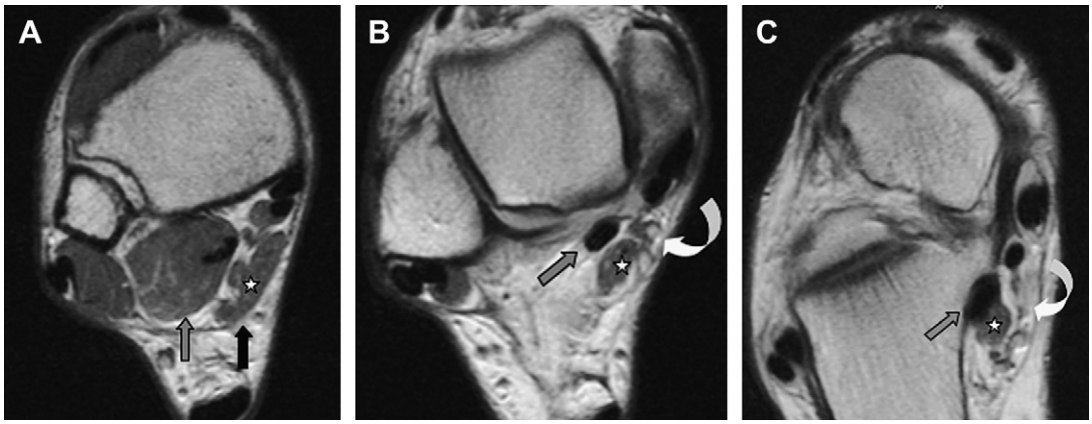

Fig. 10. Axial proton density–weighted images (*A–C*) of the ankle demonstrate an accessory flexor digitorum longus (*asterisk*) emanating proximally from the flexor retinaculum (*black arrow*) and extending alongside to the flexor hallucis longus muscle and tendon (*gray arrow*) and posterior neurovascular bundle (*curved arrow*).

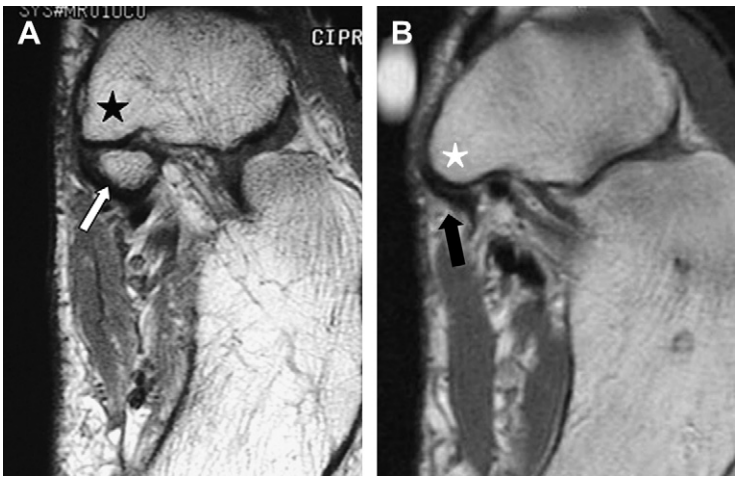

Fig. 11. Axial intermediate images demonstrate a type II navicular (*arrow*) articulating to the medial navicular tubercle (*star*) (*A*) and the posterior tibial tendon (*black arrow*) inserting onto a cornuate navicular (*white star*) (*B*).

This ossicle is bipartite or tripartite in 25% of cases.[32] Painful os peroneum syndrome presents clinically as tenderness along the lateral side of the foot at the level of the calcaneocuboid joint and is characterized on MR imaging by edematous changes in the ossicle and surrounding tendon fibers. It has a variety of causes, including fracture, peroneus longus tendon tear, and entrapment by an enlarged peroneal tubercle.[33]

Differentiation between a multipartite os peroneum and fractured os peroneum can be difficult. An acute fracture would demonstrate edematous changes in the ossicle and surrounding soft tissues. The fracture fragments have noncorticated, irregular margins, and the fragments should be able to fit together into the normal form and size of a regular os peroneum. The moieties of the multipartite os peroneum should have well corticated, smooth margins and the sum of the moieties would result in a much larger ossicle.

The os trigonum is found in the region of the posterior lateral talar tubercle. This ossicle usually forms a fibrocartilaginous syndesmosis with the talus and first becomes mineralized between the ages of 7 and 13. The ossification usually fuses with the talus to form the lateral tubercle of posterior talar process (Stieda process) but can remain a separate ossicle in 7% to 14% of people (**Fig. 12**).[34,35] Os trigonum syndrome is seen in patients who take part in activities that involve extreme plantar flexion, such as ballet, football, and soccer. The syndrome presents clinically with chronic posterior ankle pain, stiffness, and swelling due to the impingement of synovial and capsular tissue in between the posterior calcaneus, the os trigonum, and the posterior tibia.

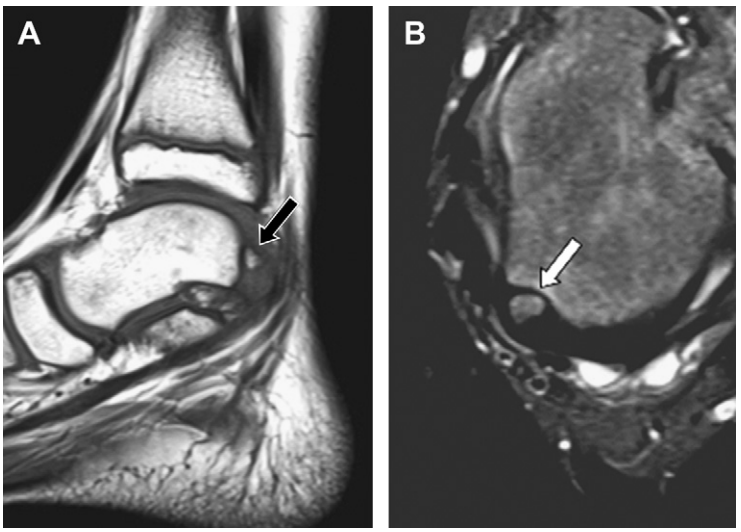

Fig. 12. Sagittal T1-weighted (*A*) and axial, fat-suppressed, T2-weighted (*B*) images demonstrate an unfused os trigonum in a skeletally immature patient (*arrows*). Note normal signal intensity within the ossification center and its synchondrosis.

MR imaging may reveal edematous changes in the posterior ankle capsule and ligaments as well as within the ossicle and posterior talus. The flexor hallucis longus tendon travels between the os trigonum and the posterior medial talar tubercle and can become inflamed, leading to chronic changes of tendinosis and/or stenosing tenosynovitis.[34] It may also be difficult to distinguish an os trigonum from a fracture of the posterior lateral talar tubercle. The irregular margins of a fracture fragment and related posttraumatic soft tissue changes can be seen on MR and CT imaging, helping distinguish between an os trigonum and a fracture of the posterior lateral talar tubercle (**Fig. 13**).[34,36]

The os intermetatarseum is an accessory ossicle found in the dorsal aspect of the midfoot between the bases of the first and second metatarsals. It can have several different shapes, including round, oval, spindle, and linear. The os intermetatarseum can form a synovial-lined joint with or become fused to an adjacent bone. Although it rarely can become symptomatic, its true importance lies in its ability to mimic a small fracture related to a Lisfranc injury. When evaluating a possible Lisfranc injury, it is important to look for other related findings, including dorsal soft tissue swelling and malalignment that help decipher between these entities.[37] The os intermetatarseum can also lead to impingement of the deep peroneal nerve as it travels dorsal to the first proximal intermetatarsal space.

The os sustentaculi is a rare accessory ossicle found at the posterior end of the sustentaculum tali along the medial aspect of the calcaneus. There is usually a fibrous or fibrocartilaginous bridge between the os sustentaculi and the calcaneus. It is best depicted in the coronal and axial planes. Familiarity with the presence of the os sustentaculi avoids the misdiagnosis of a fracture or unusual exostosis.[38]

Sesamoids

The tibial (medial) and fibular (lateral) hallucal sesamoids are found in the tendon slips of the flexor hallucis brevis and abductor hallucis muscles. Their size and shape may vary with the tibial sesamoid tending to be more elliptical whereas the fibular sesamoid tends to be more cylindrical in shape. Although both sesamoids can be partitioned, the tibial sesamoid is more frequently so. Although it has been theorized that the partitioning is due to remote trauma before ossification, this is usually a normal appearance not to be confused with fracture.[39] Bipartite hallucal ossicles have smooth and well-defined corticated margins. The sum of the proximal and distal moieties of bipartite hallucal sesamoids produces a larger-sized ossicle, which helps to distinguish a bipartite sesamoid from a fractured sesamoid. Bipartite sesamoids may be more prone to stress-related changes, including marrow edema-like pattern, fractures, and avascular necrosis.[40]

Osseous Landmarks

The retromalleolar groove is a normal shallow concavity found along the posterior aspect of the distal fibula approximately 1 cm above the tibiotalar joint that accommodates the peroneal tendons as they travel from the ankle into the foot.[41] The shape of the groove can vary from flat (11%) to convex (7%). Nonconcave shapes are thought to predispose to peroneal tendon pathology, including lateral dislocations and longitudinal tears.[42] In a recent study in asymptomatic volunteers, convex, flat, or irregular retromalleolar grooves were found in up to 72% of cases without evidence of tendon pathology.[43] Although the role

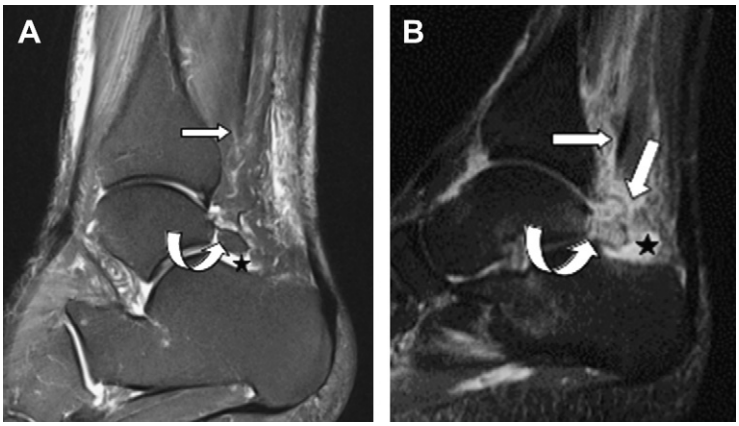

Fig. 13. (*A*) Sagittal, fat-suppressed, T2-weighted image demonstrates an os trigonum (*curved white arrow*) in an adult patient exhibiting normal internal marrow signal. Note fluid in the posterior subtalar joint recess (*asterisk*) and normal flexor hallucis longus tendon (*straight white arrow*). (*B*) Oblique, sagittal, STIR image shows a markedly edematous os trigonum (*curved arrow*) associated with posterior subtalar joint effusion (*asterisk*) as well as flexor hallucis longus strain and tenosynovitis (*straight white arrows*).

of the retromalleolar groove is in question, the authors believe it is still important to carefully evaluate the peroneal tendons and the superior peroneal retinaculum for peroneal tendon dysfunction and superior peroneal retinacular injury whenever a nonconcave fibular retromalleolar groove is encountered.

The lateral wall of the calcaneus may have an undulating configuration due to the presence of two osseous protuberances. Along the anterior aspect of the lateral calcaneal wall, the peroneal tubercle can be seen in 40% of normal individuals contributing to the peroneal tendon fibro-osseous wall along the calcaneus (**Fig. 14**). More posteriorly, a more broad-based retrotrochlear eminence is seen in 98% of the general population (**Fig. 15**). These osseous structures can grow overtime and cause problems for patients and radiologists. A hypertrophied peroneal tubercle or retrotrochlear eminence can mimic an osteochondroma or even a healing fracture. A prominent peroneal tubercle can cause mechanical friction on the adjacent peroneal longus tendon and/or peroneus brevis tendon, leading to tears and/or tenosynovitis.[44] In addition, symptomatic adventitial bursitis may develop in the vicinity of the peroneal trochlea and/or retrotrochlear eminence.[45]

Pseudocoalition

The two most common coalitions in the ankle are the subtalar and calcaneonavicular types. The coalitions can be fibrous, cartilaginous, or osseous in nature. Tarsal coalitions can be sources of chronic ankle and foot pain. The subtalar coalition is often seen at the middle subtalar joint and can be differentiated from the normal joint by its irregular opposing margins and its medial to lateral downward slope (**Fig. 16**). In addition, the sustentaculum talus tends to be deformed. True subtalar coalition should be distinguished from pseudocoalition of the medial subtalar joint.[4] A subtalar pseudocoalition is depicted on coronal and sometimes axial images as an osseous bar between the talus and the calcaneus, which is traversed by a vague, low-signal, linear shadow migrating from a cranial to caudal location on sequential images (**Fig. 17**). This appearance reflects partial volume averaging generated by the obliquity of

Fig. 14. Axial proton density–weighted image demonstrates an enlarged peroneal tubercle (*black arrow*) interposed between the peroneus brevis tendon (*white arrow*) and the peroneus longus tendon (*curved arrow*).

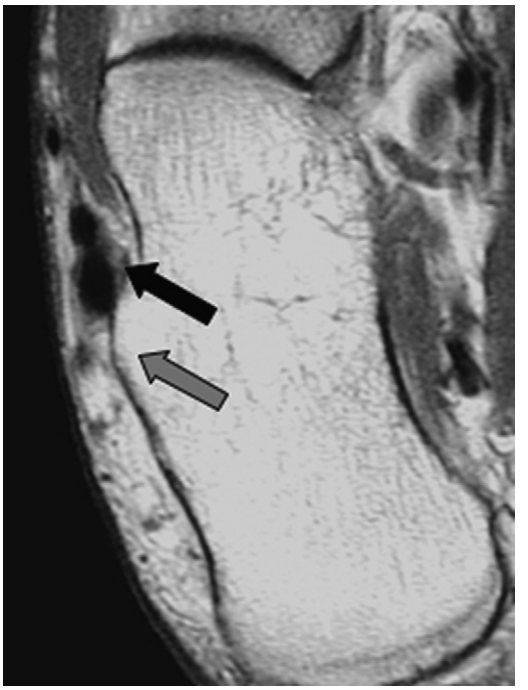

Fig. 15. Axial T1-weighted image of the ankle demonstrates a retromalleolar tubercle (*gray arrow*) along the posteromedial aspect of the peroneal tendons (*black arrow*).

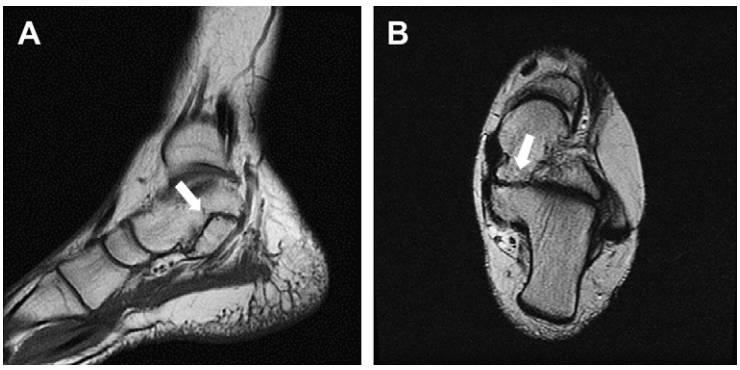

Fig. 16. Sagittal T1-weighted (*A*) and axial (*B*) fast spin-echo T2-weighted images demonstrate a fibrous subtalar coalition affecting the middle facets of the talus and calcaneus (*arrows*).

the medial subtalar joint relative to the orthogonal coronal or axial planes. This partial volume averaging is not infrequently encountered on routine axial CT images. The presence of a normal medial subtalar joint and sustentaculum talus on sagittal MR images aids in distinguishing a pseudocoalition from true coalition.

An osseous coalition between the calcaneus and the navicular bone is often simulated on sagittal T1-weighted images of the hindfoot. This pitfall can be easily avoided by noting a normal relationship between the two bones on axial and coronal images. Also, in the absence of a true coalition, gradient-echo or STIR sagittal images demonstrate bright signal between the calcaneus and navicular precluding the existence of a calcaneonavicular bar (**Fig. 18**).

The presence of a normal articulation between the navicular and cuboid has been reported in up to 45% of cadaveric ankles.[46] Therefore, the presence of articulating margins on axial images between the navicular and the cuboid should not be interpreted as coalition. This is in contradistinction to the calcaneus and navicular, which should not have articulating margins on axial images.

Pseudolesions

Pseudo-osteochondral defects are seen in the tibial plafond and the talus. The confluence of cortical trabeculae at the normal elevation of the posterior distal tibial articular surface can occasionally form a linear focus of hypointense signal in the far posterior coronal MR images of the plafond.[47] A normal groove located in the posterior aspect of the talus housing the posterior talofibular ligament can mimic an osteochondral lesion or erosion.[48] A curvilinear hypointense band produced by the insertion of the tibiotalar ligament onto the central talus can produce a pseudodefect in the subchondral bone or a few millimeters below the articular surface.

The normal multifaceted, asymmetric shape of the metatarsal bases can produce apparent articular incongruency on MR imaging, leading to the false impression of subluxation, particularly at the tarsometatarsal joint. This pitfall may lead to the misdiagnosis of a Lisfranc injury.[49] Familiarity with the typical location of these pseudolesions as well as lack of associated findings, such as soft tissue or bone marrow edema, help radiologists avoid misinterpreting normal anatomy for pathology.

Bone Marrow

Marrow edema-like signal defined as focal areas of ill-defined hypointensity on T1 and bright patchy T2 signal on fluid-sensitive sequences is a nonspecific MR finding that can be secondary to several different causes, including hematopoietic marrow reconversion, infection, trauma, and tumor. Several factors need to be considered in some cases to differentiate between these various causes, including age, distribution, and adjacent soft tissue and bone findings. Foci of high T2 signal in a starry-night pattern can be seen in the talus and calcaneus in asymptomatic patients, usually below the age of 15. These foci are thought to be caused by perivascular foci of red marrow, physiologic stress, or increased bone turnover related to weight bearing or normal skeletal growth.[50,51]

High T2 signal round/ovoid foci can also be regularly seen in the anterior calcaneus at the angle of Gissane.[52] These foci are thought to represent nutrient channels or intraosseous ganglion cysts (**Fig. 19**).[53,54] Similar-appearing high T2 foci are seen in the dorsal aspect of the talar neck and along the plantar sinus tarsi surface, which are also thought to represent vessels. Finally, high T2 signal foci can also be seen at

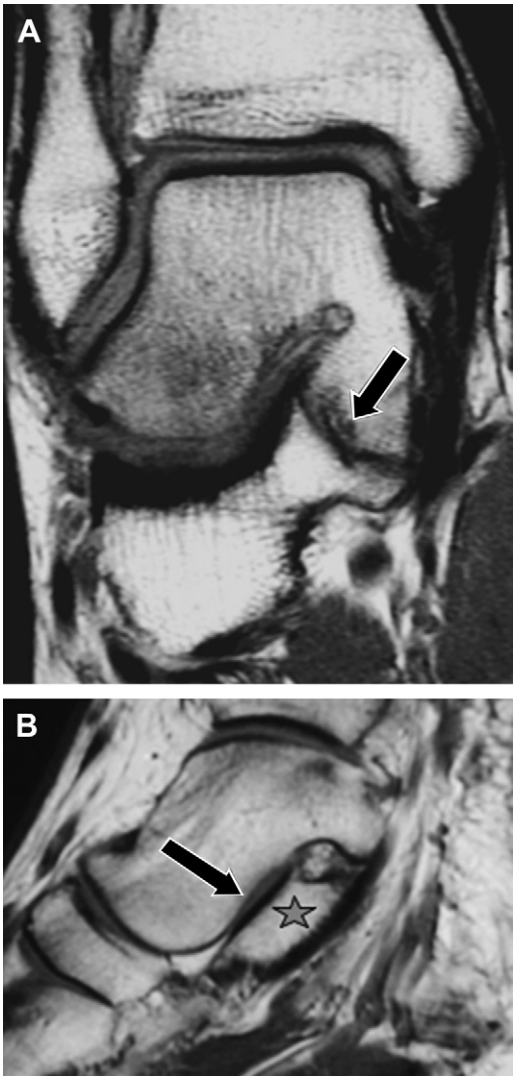

Fig. 17. Coronal T1-weighted image (*A*) of the ankle demonstrates a low signal area traversing an osseous bar in the middle subtalar joint that gives the appearance of a coalition (*black arrow*). Note the normal middle talar (*black arrow*) and calcaneal (*star*) facets of the subtalar joint on the sagittal T1-weighted image (*B*) consistent with a pseudocoalition.

several different ligament and tendon attachments, most commonly in the posterior talus and fibular notch at the attachments of the posterior talofibular ligament (Fig. 20).

Bone marrow edema pattern has also been described within the first 12 weeks after immobilization treatment after an injury. This pattern was not found to correlate with new pain or the clinical syndrome of reflex sympathetic dystrophy. Resolution or stabilization of this

Fig. 18. Sagittal T1-weighted image demonstrates a fibrous calcaneonavicular coalition (*arrow*).

bone marrow edema should be expected by 18 weeks after immobilization.[55]

Transient Physiologic MR Imaging Findings

Bursae are anatomic cushions or sacs that facilitate motion between apposing tissues.[56] They are classified into three main types: congenital, anatomic, and adventitial. Congenital bursae develop in utero and are synovial lined. Anatomic bursae develop in children at sites of normal friction, whereas

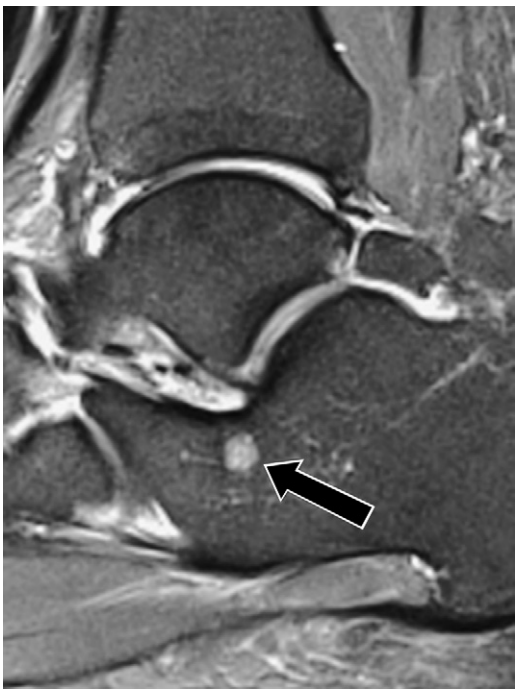

Fig. 19. Sagittal, fat-suppressed, T2-weighted image demonstrates a pseudocyst in the calcaneus just inferior to the critical angle of Gissane (*arrow*).

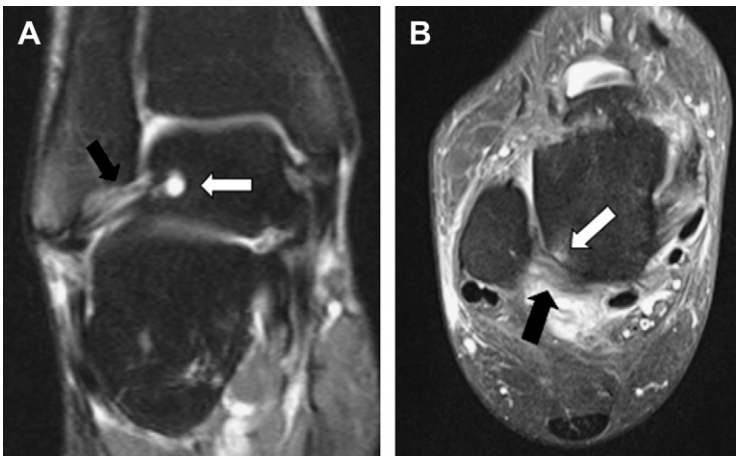

Fig. 20. (*A*) Coronal, fat-suppressed, T2-weighted image of the ankle demonstrate a traction cyst (*white arrow*) at the talar attachment of the posterior talofibular ligament (*black arrow*). (*B*) Axial, fat-suppressed, T2-weighted image demonstrates reactive marrow edema (*white arrow*) at the site of insertion of a partly torn posterior tibiofibular ligament (*black arrow*) in the setting of posterior ankle impingement.

adventitial bursae develop in adults secondary to chronic friction between soft tissues and adjacent osseous structures. Anatomic and adventitial bursae are not synovial lined. Adventitial bursae can be found throughout the foot and ankle and are usually formed adjacent to osseous protuberances.[57–61] Common locations include adjacent to the medial and lateral malleoli (**Fig. 21**), plantar surfaces of the metatarsal heads, and medial surface of the first metatarsal head. The superficial Achilles bursa is an example of an adventitial bursa that does not develop next to an osseous protuberance. Instead, it tends to develop as a result of chronic inflammation of the Achilles tendon in disorders, such as Haglund syndrome.[62] An example of a congenital bursa is the retrocalcaneal bursa, which is located between the Achilles tendon and posterosuperior aspect of the calcaneus. A small amount of physiologic fluid can be seen in this bursa normally after some activity.[63] It also can become inflamed secondary to inflammatory arthropathies, such as rheumatoid arthritis, because of its synovial lining as well as from chronic friction with the adjacent calcaneus and Achilles tendon.[60]

Transient physiologic MR imaging findings can be seen in the ankle and foot after physical activity that can mimic pathologic conditions. Fluid can be seen in the ankle joint, retrocalcaneal bursa, and the tendon sheaths, most commonly in the flexor hallucis longus. Bone marrow edema can also be occasionally present, especially after strenuous activity.[64] Physiologic fluid can be present in the first three intermetatarsal bursae in asymptomatic patients. Morton neuromas have also been found in 30% of asymptomatic subjects. It has been speculated that these neuromas

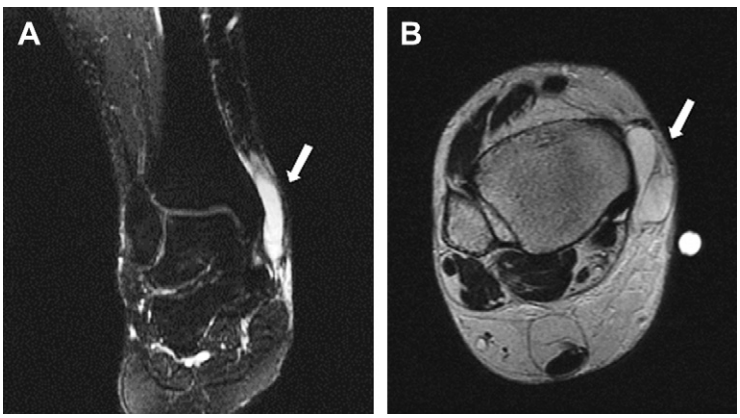

Fig. 21. Coronal, fat-suppressed, T2-weighted (*A*) and axial, fast spin-echo, T2-weighted (*B*) images demonstrate medial malleolar bursitis (*arrows*).

may only become relevant when they reach a transverse diameter of 5 mm or more. Correlation with patient clinical history and physical examination is recommended.[65,66]

REFERENCES

1. Ouzounian TJ, Anderson R. Anterior tibial tendon rupture. Foot Ankle Int 1995;16:406–10.
2. Mengiardi B, Pfirrmann CW, Vienne P, et al. Anterior tibial tendon abnormalities: MR imaging findings. Radiology 2005;235:977–84.
3. Erickson SJ, Cox IH, Hyde JS, et al. Effect of tendon orientation on MR imaging signal intensity: a manifestation of the "magic angle" phenomenon. Radiology 1991;181:389–92.
4. Rosenberg ZS, Bencardino J, Mellado JM. Normal variants and pitfalls in magnetic resonance imaging of the foot and ankle. Top Magn Reson Imaging 1998;9:262–72.
5. Delfaut EM, Demondion X, Bieganski A, et al. The fibrocartilaginous sesamoid: a cause of size and signal variation in the normal distal posterior tibial tendon. Eur Radiol 2003;13:2642–9.
6. Schweitzer ME, Van Leersum M, Ehrlich SS, et al. Fluid in normal and abnormal ankle joints: amount and distribution as seen on MR Images. Am J Roentgenol 1994;162:111–4.
7. Mantel D, Falutre B, Bastian D, et al. [Structural MRI study of the Achilles tendon: correlation with microanatomy and histology]. J Radiol 1996;77:261–5 [in French].
8. Schweitzer ME, Karasick D. MR imaging of disorders of the posterior tibial tendon. Am J Roentgenol 2000;175:627–35.
9. Soila K, Karjalainen PT, Aronen HJ, et al. High resolution MR imaging of the asymptomatic Achilles tendon: new observations. Am J Roentgenol 1999; 173:323–8.
10. Mellado JM, Rosenberg ZS, Beltran J, et al. Low incorporation of the soleus tendon: MR interpretation pitfall. Skeletal Radiol 1998;27:222–4.
11. Schweitzer ME, Karasick D. MR imaging of disorders of the Achilles tendon. Am J Roentgenol 2000;175:613–25.
12. Bude RO, Adler RS, Bassett DR. Diagnosis of Achilles Tendon Xanthoma in patients with heterozygous familial hypercholesterolemia: MR vs Sonography. Am J Roentgenol 1994;162:913–7.
13. Wang XT, Rosenberg ZS, Mechlin MB, et al. Normal variants and diseases of the peroneal tendons and superior peroneal retinaculum: MR imaging features. Radiographics 2005;25:587–602.
14. Noto AM, Cheung Y, Rosenberg ZS, et al. MR imaging of the ankle: normal variants. Radiology 1989;170:121–4.
15. Mengiardi B, Pfirrman CW, Vienne P. Medial collateral ligament complex of the ankle: MR appearance in asymptomatic subjects. Radiology 2007;242:817–24.
16. Mengiardi B, Zanetti M, Schottle PB, et al. Spring ligament complex: MR imaging-anatomic correlation and findings in asymptomatic subjects. Radiology 2005;237:242–9.
17. Desai K, Beltran L, Bencardino J, et al. The spring recess of the anterior subtalar joint: depiction on MR images with cadaveric correlation. Accepted for presentation at the 2010 ARRS annual meeting. San Diego (CA), May 2–7, 2010.
18. Oh CS, Won HS, Hur MS, et al. Anatomic variations and MRI of the intermalleolar ligament. Am J Roentgenol 2006;186:943–7.
19. Rosenberg ZS, Cheung Y, Beltran J, et al. Posterior intermalleolar ligament of the ankle: normal anatomy and MR imaging features. Am J Roentgenol 1995; 165:387–90.
20. Buschmann WR, Cheung Y, Jahss MH. Magnetic resonance imaging of anomalous leg muscles: accessory soleus, peroneus quartus and the flexor digitorum longus accessorius. Foot Ankle 1991;12: 109–16.
21. Rosenberg ZS, Bencardino J, Cheung YY, et al. Normal muscle variants of the ankle. Radiology 1997;205(P):645.
22. Cheung YY, Rosenberg ZS, Ramsinghani R, et al. Peroneus quartus muscle: MR imaging features. Radiology 1997;202:745.
23. Cheung YY, Rosenberg ZS, Colon E, et al. MR imaging of the accessory flexor digitorum longus tendon. Skeletal Radiol 1999;28:130–7.
24. Ekstrom JE, Shuman WP, Mack LA. MR imaging of accessory soleus muscle. J Comput Assist Tomogr 1990;14:239–42.
25. Yu JS, Resnick D. MR Imaging of the accessory soleus muscle appearance in six patients and a review of the literature. Skeletal Radiol 1994;23:525–8.
26. Romanus B, Lindahl S, Stener B. Accessory soleus muscle. A clinical and radiographic presentation of eleven cases. J Bone J Surg 1986;68:731–4.
27. Lawson JP. Not so normal variants. Orthop Clin North Am 1990;21:483–95.
28. Miller TT, Staron RB, Feldman F, et al. The symptomatic accessory tarsal navicular bone: assessment with MR imaging. Radiology 1995;195:849–53.
29. Bernaerts A, Vanhoenacker FM, Van de Perre S, et al. Accessory navicular bone: not such a normal variant. Belgian J Radiol 2004;87:250–2.
30. Lovejoy CO, Latimer B, Suwa G, et al. Combining prehension and propulsion: the foot of *Ardipithecus ramidus*. Science 2009;326:72, 72e1–72e8.
31. Le Minor JM. Comparative anatomy and significance of the sesamoid bone of the peroneus longus muscle (os peroneum). J Anat 1987;151:85–99.

32. Mota JM, Rosenberg ZR. Magnetic resonance imaging of the peroneal tendons. Top Magn Reson Imaging 1998;9:273–85.
33. Sobel M, Pavlov H, Geppert MJ, et al. Painful os peroneum syndrome: a spectrum of conditions responsible for plantar lateral foot pain. Foot Ankle Int 1994;15:112–24.
34. Karasick D, Schweitzer ME. The os trigonum syndrome: imaging features. Am J Roentgenol 1996;166:125–9.
35. Lawson JP. Clinically significant radiologic anatomic variants of the skeleton. Am J Roentgenol 1994;163: 249–55.
36. Karasick D. Fractures and dislocations of the foot. Semin Roentgenol 1994;29:152–75.
37. Mellado JM. Accessory ossicles and sesamoid bones of the ankle and foot: imaging findings, clinical significance and differential diagnosis. Eur Radiol 2003;12:L164–77.
38. Bencardino J, Rosenberg ZS, Beltran J, et al. Os sustentaculi: depiction on MR images. Skeletal Radiol 1997;26:505–6.
39. Karasick D, Schweitzer ME. Disorders of the hallux sesamoid complex: MR features. Skeletal Radiol 1998;27:411–8.
40. Taylor J, Sartoris DJ, Huang G, et al. Painful conditions affecting the first metatarsal Sesamoid bones. Radiographics 1993;13:817–30.
41. Edwards ME. The relations of the peroneal tendons to the fibula, calcaneus, and cuboideum. Am J Anat 1928;42:213–53.
42. Rosenberg ZS, Beltran J, Cheung YY, et al. MR features of longitudinal tears of the peroneus brevis tendon. Am J Roentgenol 1997;168:141–7.
43. Saupe N, Mengiardi B, Pfirrmann C, et al. Anatomic variants associated with peroneal tendon disorders: MR imaging findings in volunteers with asymptomatic ankles. Radiology 2007;242:509–17.
44. Thompson FM, Patterson AH. Rupture of the peroneus longus tendon. J Bone Joint Surg Am 1989; 71-A:293–5.
45. Boles MA, Lomasney LM, Demos TC. Enlarged peroneal process with peroneus longus tendon entrapment. Skeletal Radiol 1997;26:313–5.
46. Sarrafian S. Anatomy of the foot and ankle. 2nd edition. Philadelphia: Lippincott; 1993.
47. Pomerantz SJ, Kim TW. Pitfalls and variations in neuro orthopaedic MRI. Cincinnati (OH): MRI-EFI Publications; 1995. 6.1–6.54.
48. Miller TT, Bucchieri JS, Joshi A, et al. Pseudodefect of the talar dome: an anatomic pitfall of ankle MR imaging. Radiology 1997;203:857–8.
49. Delfault EM, Rosenberg ZS. Step off and incongruities at Lisfranc joint in asymptomatic individuals: MR imaging features. Radiology 1998;209:345.
50. Shabshin N, Schweitzer ME, Morrison W. High-signal T2 changes of the bone marrow of the foot and ankle in children: red marrow or traumatic changes? Pediatr Radiol 2006;36:670–6.
51. Laor T, Jaramillo D. MR imaging insights into skeletal maturation: what is normal? Radiology 2009;250:28–38.
52. Zubler V, Mengiardi B, Pfirrmann CW, et al. Bone marrow changes on STIR MR images of asymptomatic feet and ankles. Eur Radiol 2007;17:3066–72.
53. Elias I, Zoga AC, Raikin SM, et al. Incidence and morphologic characteristics of benign calcaneal cystic lesions on MRI. Foot Ankle Int 2007;28: 707–14.
54. Fleming JL 2nd, Dodd L, Helms CA. Prominent vascular remnants in the calcaneus simulating a lesion on MRI of the ankle: findings in 67 patients with cadaveric correlation. Am J Roentgenol 2005; 185:1449–52.
55. Elias I, Zoga AC, Schweitzer ME, et al. A specific bone marrow edema around the foot and ankle following trauma and immobilization therapy: pattern description and potential clinical relevance. Foot Ankle Int 2007;28:463–71.
56. Resnick D, Kransdorf MJ. Bone and joint imaging. 3rd edition. Philadelphia: Elsevier Saunders; 2005. p. 975.
57. Jahss MH. Miscellaneous soft-tissue lesions. In: Jahss MH, editor. Disorders of the foot and ankle: medical and surgical management. 2nd edition. Philadelphia: Saunders Company; 1991. p. 1514–39.
58. Hernandez PA. Clinical aspects of bursae and tendon sheaths of the foot. J Am Podiatr Med Assoc 1991;81:366–72.
59. Hartmann. The tendon sheaths and synovial bursae of the foot. Foot Ankle 1981;1:247–69.
60. Sarrafian SK. Tendon sheaths and bursae. In: Sarrafian SK, editor. Anatomy of the foot and ankle: descriptive, topographic, functional. 2nd edition. Philadelphia: Lippincott; 1993. p. 283–93.
61. Brown RR, Rosenberg ZS, Schweitzer ME. MRI of the medial malleolar bursa. Am J Roentgenol 2005; 184:979–83.
62. Pavlov HP, Heneghan MA, Hersh A. The Haglund syndrome: initial and differential diagnosis. Radiology 1982;144:83–8.
63. Pfirrman CW, Zanetti M, Hodler J. Joint MR imaging: normal variants and pitfalls related to sports injury. Magn Reson Imaging Clin N Am 2003;11:193–205.
64. Lohman M, Kivisaari A, Vehmas T, et al. MR imaging abnormalities of foot and ankle in asymptomatic, physically active individuals. Skeletal Radiol 2001; 30:61–6.
65. Zanetti M, Strehle KL, Zollinger H, et al. Morton neuroma and fluid in the intermetatarsal bursae on MR images of 70 asymptomatic volunteers. Radiology 1997;203:516–20.
66. Bencardino J, Rosenberg ZS, Beltran J, et al. Morton's neuroma: is it always symptomatic? Am J Roentgenol 2000;175:649–53.